

may produce a functional deficit in the central nervous system in the absence of any overt toxicity. Compelling preliminary evidence supporting the seriousness of this functional deficit has been noted in adult rats exposed to CO as fetuses (16). Although no impairment was observed in avoidance acquisition, young adult rats prenatally exposed to CO demonstrated impaired retention as indexed by reacquisition. While we cannot extrapolate the results to humans, they do resemble the often cited impairment in achievement test scores noted during early childhood in the children of women who were heavy smokers during pregnancy (17). Further research identifying the underlying neural substrates for such behavioral alterations may permit extrapolation across species.

CHARLES F. MACTUTUS*
LAURENCE D. FECHTER

Neurotoxicology Program,
Department of Environmental Health
Sciences, Johns Hopkins University,
Baltimore, Maryland 21205

References and Notes

1. J. S. Haldane, *J. Physiol. (London)* **18**, 430 (1895).
2. V. G. Laties and W. H. Merigan, *Annu. Rev. Pharmacol. Toxicol.* **19**, 357 (1979); L. D. Longo, *Am. J. Obstet. Gynecol.* **137**, 162 (1980).
3. National Research Council, *Report of the Committee on Medical and Biologic Effects of Environmental Pollutants* (National Academy of Sciences, Washington, D.C., 1977).
4. L. D. Longo, *Ann. N.Y. Acad. Sci.* **174**, 313 (1970); *Science* **194**, 523 (1976); _____ and E. P. Hill, *Am. J. Physiol.* **232**, H324 (1977).
5. B. A. Schwetz, F. A. Smith, B. K. J. Leong, R. E. Staples, *Teratology* **19**, 385 (1979).
6. P. Astrup, H. Olsen, D. Trolle, K. Kjeldsen, *Lancet* **1972-II**, 1220 (1972).
7. L. D. Fechter and Z. Annau, *Science* **197**, 680 (1977); *Neurobehav. Toxicol.* **2**, 7 (1980).
8. HbCO levels were determined using the spectrophotometric method of K. Small *et al.* [*J. Appl. Physiol.* **31**, 154 (1971)].
9. J. Goldsmith, *Ann. N.Y. Acad. Sci.* **174**, 122 (1970); P. Lawther and B. Commins, *ibid.* p. 135; P. Coles, *Nature (London)* **255**, 699 (1975); A. Kahn *et al.*, *Arch. Environ. Health* **29**, 127 (1974).
10. The two-way active avoidance task was chosen for the behavioral procedure because the functional ontogeny for this particular task appears to span a broader developmental period [R. H. Bauer, *Dev. Psychobiol.* **11**, 103 (1978)] than either a one-way active [D. A. Feigley and N. E. Spear, *J. Comp. Physiol. Psychol.* **73**, 515 (1970)] or passive avoidance procedure [D. C. Riccio, M. Rohrbaugh, L. A. Hodges, *Dev. Psychobiol.* **1**, 108 (1968)].
11. Avoidance training was given in a commercially available two-compartment shuttle box (27 by 11 by 13 cm) in which the spacing of the floor grids was modified to accommodate rats of the three ages. Each trial began with the presentation of a compound light-tone stimulus followed 5 seconds later by the onset of the unconditioned footshock stimulus (1.0 mA constant current) delivered to both the walls and floor of the compartment in which the trial began. If the rats did not make an avoidance response during the first 5 seconds of the trial, the mildly aversive shock stimulus was initiated and remained on until an escape was made or until 30 seconds had elapsed.
12. Analyses subsequent to a significant *F* value were performed with the conservative Bonferroni or Dunn's test to maintain the overall alpha level within any set of contrasts at the probability level of $P < 0.05$ [B. J. Winer, *Statistical Principles in Experimental Design*, (McGraw-Hill, New York, ed. 2, 1971)].
13. Moreover, analyses of covariance used to correct for the minor differences in initial escape latencies and responding during an intertrial interval (adaptation responding also included in the replication experiment) confirmed a significant impairment in the offspring of CO-exposed dams and indicated an associative deficit.

14. C. F. Flaherty *et al.*, *Learning and Memory* (Rand McNally, Chicago, 1977).
15. All sessions contained 100 trials and began with a 5-minute adaptation period. For the learning-memory and maturation control conditions, the intertrial interval was a variable 60-second schedule (35 to 85 seconds); for the random control condition, either a conditional or unconditional stimulus occurred, on average, every 30 (5 to 55) seconds. This random procedure was conservative in retaining an avoidance contingency which, if met, precluded delivery of the next scheduled shock.

16. C. F. Mactutus and L. D. Fechter, in preparation.
 17. R. Davie, N. Butler, H. Goldstein, *From Birth to Seven: The Second Report of the National Child Development Study* (Longman, London, 1972).
 18. Funded in part by NIH grants ES01589 and ES07094 and by grant R-80906101-0 from the Environmental Protection Agency. We gratefully acknowledge the support and laboratory facilities provided by Z. Annau and the technical assistance of R. Lintz and J. Campbell with computer hardware and software, respectively.
- * Present address: Laboratory of Behavioral and Neurological Toxicology, National Institute of Environmental Health Sciences, P.O. Box 12233, Research Triangle Park, N.C. 27709.

26 September 1983; accepted 13 October 1983

Rapid Mechanical Responses of the Dark-Adapted Squid Retina to Light Pulses

Abstract. Dark-adapted squid retinas respond to brief light pulses with early and late mechanical responses. These responses are mechanical counterparts of the early and late receptor potentials.

Photomechanical responses of the retina—movements of visual cells and pigments produced by light—have been known to physiologists for more than a century (1). By comparing the photomicrographs of the retinas prepared in light-adapted and dark-adapted states, Young (2) showed that the photoreceptors in the octopus and squid eye “contract” when exposed to light. The sensitivity of the microscopic method for detecting mechanical movements in the retina is limited.

We have found that rapid mechanical responses to light stimuli can be detected with a piezoelectric transducer pressing onto dark-adapted squid retina. Previously, rapid mechanical movements were detected by the use of the same transducer in crab nerves, in squid giant

axons, and in frog dorsal-root ganglia and spinal cords (3).

Squid, *Loligo pealeii* Lesueur, were used. After about 60 minutes of dark adaptation, the eye was excised under illumination with dim red light and transferred into oxygenated artificial seawater. The cornea and the lens of the eye were then resected with a pair of fine scissors, and a disk of the retina of about 12 mm in diameter was prepared. Finally, the retina was transferred into oxygenated seawater in a black Lucite chamber (Fig. 1). The chamber consisted of two compartments separated by a partition provided with a short tube fixed vertically in the middle. The opening of the tube was completely covered with the retina, whose internal limiting membrane faced upward. The retinal surface was fixed with a separate Lucite ring with a hole 4 mm in diameter in the middle. After the hydrostatic pressure in the closed lower compartment was slightly raised, the stylus of a piezoelectric probe was lowered to make contact with the center of the retina.

The piezoelectric probe was of the lead-zirconate-titanate type (Gulton) connected to an operational amplifier (AD 515); its sensitivity was roughly 30 mV per milligram. The output was amplified by a factor of 100 in the frequency range between 0.1 and 300 Hz and was led to a dual-beam oscilloscope, a signal averager, or both. Variations in the electric potential difference across the retina evoked by light pulses [that is, electroretinogram (ERG)] were recorded with a pair of electrodes, one chloridized silver wire in each compartment. All measurements were carried out at room temperature (19° to 21°C).

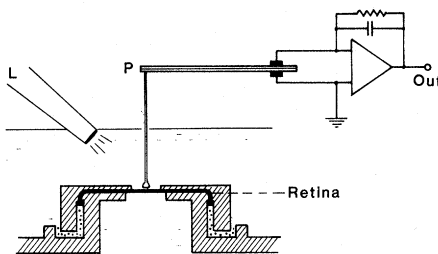


Fig. 1. Schematic diagram of the experimental setup used for measuring photomechanical movements of the squid retina. The retina was clamped between two plastic rings with holes in the middle. The shaded areas represent the partition and the rings dividing the seawater into two parts. The stippled areas represent the space filled with Vaseline. The Ag-AgCl electrode (not shown) immersed in seawater above the partition was grounded; an electrode in the lower compartment recorded the ERG. Abbreviations: L, light-emitting diode operated at 3 V (100 mA); P, piezoelectric transducer connected to an operational amplifier.

The set of digitized records in Fig. 2 is an example of photomechanical responses taken from an isolated piece of the retina (detached from the sclera), displayed with the ERG. These responses were evoked by light pulses generated by a 0.3-W light-emitting diode placed about 7 mm from the center of the retina. The wavelength of maximum emission of the diode was 565 nm, and its half-band-

width was 26 nm; in the absence of the probe, the light intensity at the plane of the retina was estimated to be $50 \mu\text{W}/\text{cm}^2$.

An upward deflection of the top trace in these records indicates that the retina developed a force tending to move the probe upwards. Small negative mechanical deflections with an extremely short latency started nearly simultaneously

with the onset of the light pulse and were insensitive to both anoxia and light adaptation. These short-latency responses seem to represent mechanical counterparts of the early receptor potentials (4).

The late mechanical response was diphasic, a brief (and small) positive deflection followed by a long (and large) negative deflection (Fig. 3). When the stylus of the probe was pressing the retinal lightly, the amplitude of the early mechanical response was usually far smaller than that of the late responses. The peak of the positive mechanical response preceded that of the ERG.

With light pulses of 5 to 7 msec, the positive mechanical response started shortly before the end of the light pulse and lasted 30 to 50 msec. Its amplitude varied between 3 and $14 \mu\text{g}$ depending on the method of preparing the retina, as well as on the initial pressure applied to the retina with the stylus. Since the foot-plate of the stylus was roughly 1 mm in diameter, a positive deflection of $8 \mu\text{g}$ corresponds to a pressure rise of about one dyne/cm². The duration of the large negative phase was comparable to that of the ERG.

An important aspect of the mechanical responses was revealed when the effect of light adaptation was examined. When the room light was turned on, the amplitudes of both the late mechanical response and the ERG were immediately reduced (Fig. 3B). When the room light was turned off again, both late mechanical and electrical responses to brief light pulses recovered gradually (Fig. 3, C and D).

In the squid retina, the outer (distal) segments of the photoreceptors form a thick, compact layer underneath the internal limiting membrane (5). Both the early mechanical responses and the positive phase of the late mechanical response are probably generated in this layer by activities of the rod outer segment membrane (6). The late negative component of the mechanical response, which represents a decrease in the thickness of the retina, is expected to pass into the contraction described by Young (2) when the light stimulus is maintained.

We have carried out similar observations by placing lobster eyestalks in the chamber (Fig. 1) and illuminating the corneal surface from below. We have also examined the wavelength dependence of the mechanical response by using several types of light-emitting diodes as well as a series of optical filters in conjunction with a source of flash-light. The results of these observations are consistent with our interpretation of the phenomena described above.

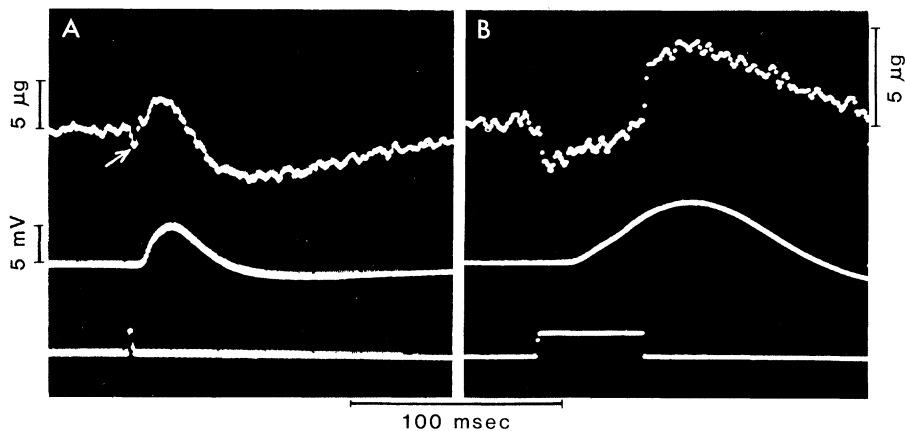


Fig. 2. Digitized records of mechanical responses (averaged over eight trials repeated at about 4-second intervals) taken from a dark-adapted squid retina detached from the sclera. The ERG is shown below. (A) The early photomechanical response (produced by a 4-msec light pulse) is indicated by the arrow. (B) The late photomechanical response started during the course of the early response.

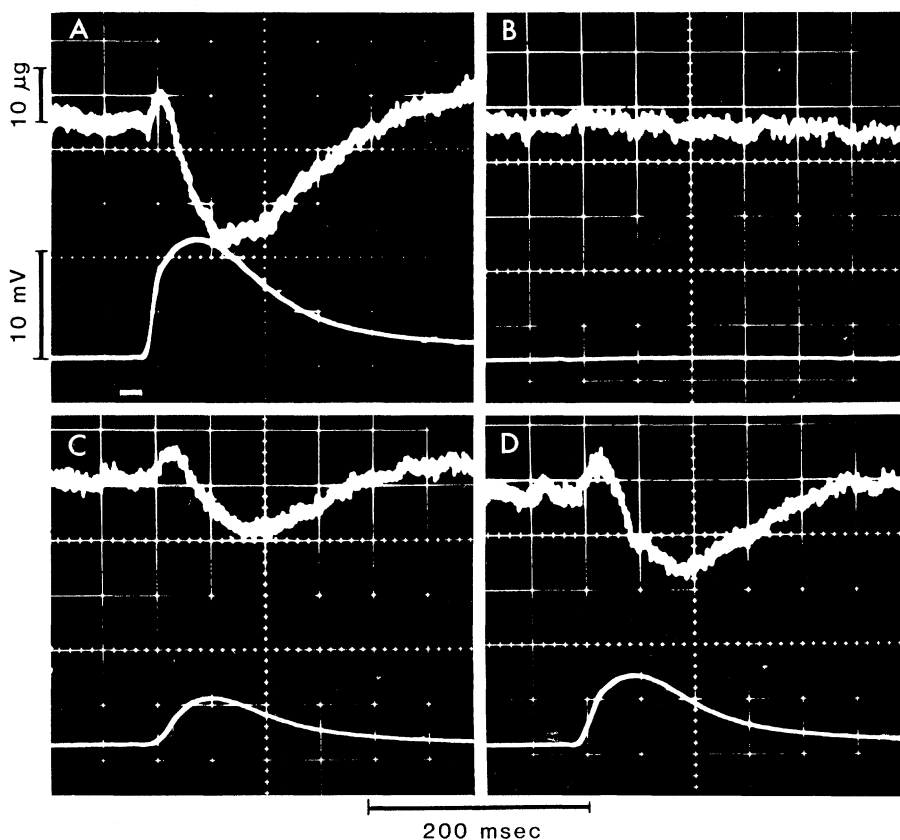


Fig. 3. Oscillograph records of photomechanical responses (top trace) and ERG (bottom trace) recorded from a squid retina with the sclera left intact. (A) Record from a dark-adapted retina. The light stimulus is indicated by the bar. (B) Record taken near the end of 30 seconds of light adaptation. (C) Record taken about 40 seconds after the resumption of dark adaptation. (D) Record taken from the same retina kept for 150 seconds in darkness.

Rapid mechanical changes have been demonstrated during excitation of almost all the excitable tissues examined. Therefore, the mechanical responses observed in the invertebrate retinas appear to be an expression of general physicochemical processes involving the plasma membrane and cytoskeleton of excitable cells.

ICHIJI TASAKI
TOSHIO NAKAYE

Laboratory of Neurobiology, National Institute of Mental Health, Bethesda, Maryland 20205 and Marine Biological Laboratory, Woods Hole, Massachusetts 02543

References and Notes

1. S. R. Detwiler, *Vertebrate Photoreceptors* (Macmillan, New York, 1943), p. 77; J. J. Wolken, in *Physical Principles of Biological Membranes*, F. Snell *et al.*, Eds. (Gordon & Breach, New York, 1969), p. 365; P. O'Connor and B. Burnside, *J. Cell Biol.* **89**, 517 (1981).
2. J. Z. Young, *Proc. Zool. Soc. London* **140**, 255 (1963).
3. K. Iwasa, I. Tasaki, R. C. Gibbons, *Science* **210**, 338 (1980); I. Tasaki, *Physiology and Electrochemistry of Nerve Fibers* (Academic Press, New York, 1982), p. 350; I. Tasaki and P. M. Byrne, *Brain Res.* **272**, 360 (1983).
4. K. T. Brown and M. Murakami, *Nature (London)* **201**, 626 (1964).
5. H. V. Zonana, *Bull. Johns Hopkins Hosp.* **109**, 185 (1961); A. I. Cohen, *J. Comp. Neurol.* **147**, 351 (1973).
6. W. A. Hagins and R. E. McLaughy, *Science* **159**, 213 (1968); W. A. Hagins, H. V. Zonana, R. G. Adams, *Nature (London)* **194**, 844 (1962).

27 October 1983; accepted 20 December 1983

Crystals of the Octameric Histone Core of the Nucleosome

Abstract. *The undegraded core histone octamer has been crystallized in a form suitable for x-ray analysis. The hexagonal bipyramidal crystals reproducibly grow larger than 1.0 by 0.6 millimeter. X-ray reflections are observed from Bragg planes with spacings larger than 3.5 angstroms. The crystals have the symmetry of the space group $P3_121$ or its enantiomorph. There appears to be one histone octamer per asymmetric unit.*

Most of the DNA in eukaryotic chromosomes is organized into repeating structural units by its interaction with a set of basic proteins called histones (1). Electron microscopy of chromatin allows visualization of a fiber (100 Å diameter) with a repeating structure that resembles a string of beads (2). Brief digestion of chromatin with micrococcal nuclease yields nucleosomes containing about 200 base pairs (bp) of DNA, two each of the four core histone molecules H2A, H2B, H3, and H4, and one molecule of histone H1 (3). A series of nucleosomes corresponds to the repeating structures observed in electron micrographs. Further digestion of chromatin with micrococcal nuclease cleaves the less tightly complexed DNA and releases H1 and yields the nucleosome core particle, which consists of 146 bp of DNA wrapped around the octameric histone core (H2A, H2B, H3, H4)₂.

Extensive analysis of nucleosome core particles and their octameric histone core by electron microscopy (4, 5), x-ray (6) and neutron diffraction (7), and chemical cross-linking (8) has yielded a picture of the nucleosome core particle to a resolution of about 25 Å. It appears to be a wedge-shaped disk 110 Å in diameter and 55 Å at its thickest edge. One-and-three-quarter turns of double-stranded DNA are wrapped around the outside of the histone octamer in a superhelix with a pitch of about 28 Å. The octamer is also a wedge-shaped disk, about 70 Å in diameter and 55 Å high, possibly with a

protruding ramp corresponding to the path of the DNA supercoil (5). To the resolution of the methods used, there is a twofold axis of symmetry in both the nucleosome core particle and the histone octamer.

The histone octamer can be extracted from chromatin as a stable undissociated particle in 2M NaCl (9, 10). In physiologic ionic strengths in the absence of DNA, the octamer dissociates into subunits: the (H3, H4)₂ tetramer and two (H2A, H2B) dimers (10). By combining the histone octamer or a mixture of the dimer and tetramer subunits with DNA under appropriate conditions, complexes that appear identical to nucleosome core par-

ticles by a number of criteria can be reconstituted (11). We have attempted to crystallize the (H2A, H2B, H3, H4)₂ histone octamer and its physiological subunits, the (H2A, H2B) dimer and the (H3, H4)₂ tetramer. We have previously reported our results with crystals of one subassembly of the core histones, the slightly proteolyzed (H3, H4)₂ tetramer from calf thymus (12). We report here the first crystals of the complete assembly of the undegraded histone octamer.

Chicken erythrocytes were obtained from Pel Freeze Biologicals. Nuclei were isolated by the method of Olins *et al.* (13). Histone octamer was isolated according to Eickbush and Moudrianakis (10). To prepare the octamer for crystallization, a concentrated (20 mg/ml) solution of pure chicken erythrocyte octamer in 2M NaCl, 1 mM EDTA, and 10 mM tris, pH 7.5, was dialyzed against 60 percent stock ammonium sulfate (70 g plus 100 ml of water), with 10 mM NaP₂O₇, pH 6.5, 5 mM EDTA, and 1 percent 2-mercaptoethanol (crystallization buffer). The next day this material was dialyzed against a 65 percent stock solution of ammonium sulfate and crystallization buffer. The following day the solution was clarified by centrifugation, and the protein in solution was placed in Zeppezaur tubes (14) and dialyzed against 67 percent stock ammonium sulfate and crystallization buffer. Crystals reproducibly grew in about 1 week and continued to grow for about 2 months. Increasing the concentration of the ammonium sulfate to 69 percent stock caused the crystals to continue to increase in size. All steps were carried out at 4°C.

The crystals are clear, nonbirefringent, hexagonal bipyramids (Fig. 1A) that grow larger than 1.0 by 0.6 mm. The

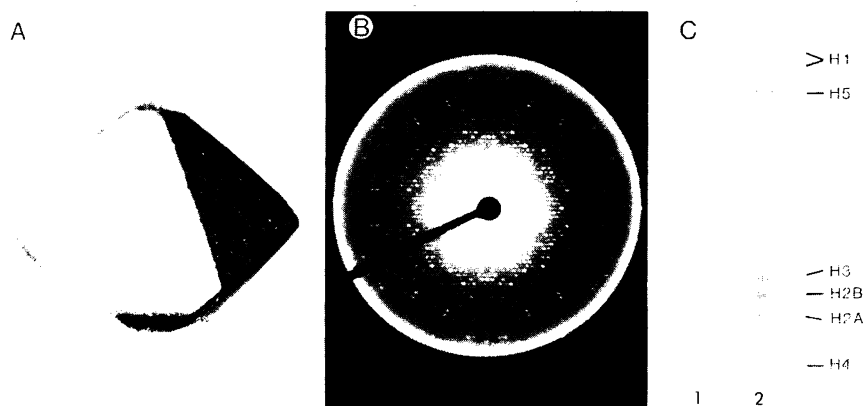


Fig. 1. (A) Light micrograph of a hexagonal bipyramidal crystal of the histone octamer that is about 0.4 by 0.5 mm. (B) A 12.5° screened precession picture of the zero layer looking down the threefold axis. Reflections at 3.5 Å resolution are apparent. (C) Photograph of sodium dodecyl sulfate-polyacrylamide gels (10); (lane 1) proteins recovered from a single crystal; (lane 2) acid-extracted chick erythrocyte total histones.